Olli Haavisto and Heikki Hyötyniemi. 2009. Reflectance spectroscopy in the analysis of mineral flotation slurries. In: Luis Bergh (editor). Pre-prints of the Workshop on Automation in Mining, Mineral and Metal Industry (IFACMMM 2009). Viña del Mar, Chile. 14-16 October 2009, 6 pages.

Reflectance Spectroscopy in the Analysis of Mineral Flotation Slurries

Olli Haavisto, **Heikki Hyötyniemi**

Helsinki University of Technology (TKK),
Department of Automation and Systems Technology,
P.O.Box 5500, FI-02015 TKK, Finland
(e-mail: olli.haavisto@tkk.fi)

Abstract: Effective monitoring and control of a mineral flotation process necessitates accurate and rapid on-line analysis of the slurry flows. Recent development of lightweight and low-cost visible and near-infrared (VNIR) imaging spectrographs has provided new interesting possibilities also in mineral froth and slurry analysis. The intelligent combination of VNIR reflectance spectroscopy with the traditional X-ray fluorescence analysis for improved measurement of the mineral slurry contents is discussed in this article. The main improvement is the radically reduced sampling interval of the analysis.

Keywords: mineral flotation, reflectance spectroscopy, X-ray fluorescence, elemental assaying, partial least squares

1. INTRODUCTION

Flotation is one of the most common mineral concentration methods used to separate valuable minerals from the waste rock (Wills and Napier-Munn, 2006). A typical flotation circuit contains several flotation stages each consisting of interconnected flotation cells. Monitoring of the flotation performance in different parts of the process is based on the elemental analysis or assaying of the slurry flows connecting the flotation stages. In most concentration plants these assays are obtained by an X-ray fluorescence (XRF) analyzer that monitors the contents of the slurries on-line. This enables the automatic control of the process (McKee, 1991).

Machine vision based analysis of the flotation froths has been studied mainly as a method to measure the general state of the flotation cells, but also as an alternative lightweight method to assay the froth (Liu et al., 2005; Bartolacci et al., 2006; Morar et al., 2005; Kaartinen et al., 2006). Especially the color information of the froth or slurry has been detected to correlate with the mineral grades (Oestreich et al., 1995; Hargrave and Hall, 1997). Consequently, the possibilities of visible and near infrared (VNIR, wavelengths between 400–1000 nm) reflectance spectroscopy of flotation froths and slurries have been investigated for improved elemental assaying (Haavisto et al., 2006, 2008). A commercial mineral analyzer apparently based on VNIR reflectance spectroscopy has also been developed (De Waal, 2007).

The development of a slurry elemental analyzer prototype which combines VNIR reflectance spectroscopy with a centralized XRF analyzer has previously been reported by (Haavisto et al., 2008) and (Haavisto and Kaartinen, 2008). The essential benefit of the VNIR spectrum based assaying is the short sampling interval obtained with respect to the cost of the equipment. A common sampling interval of a centralized XRF analyzer is around 10–20 minutes, whereas the VNIR spectrum can easily be measured and the assay calculated every five or ten seconds. This enables the fast detection of rapid changes in the slurry grades and gives the flotation process operators instant feedback for their manual control actions. The enhanced grade measurements have proven to be especially useful in detecting high-frequency grade oscillations that would normally be missed by the regular XRF analyzer because of its slower sampling speed (Haavisto, 2009).

This study reports the latest development stage of the VNIR slurry analyzer prototype and summarizes the adaptive data-based calibration used to ensure the precision of the assay. In addition, a recursive method to estimate the precision of the VNIR assay is presented and the performance of the analyzer in real copper and zinc flotation circuits is demonstrated.

2. MEASUREMENT SETUP

The slurry spectrum analyzer was developed and tested at Pyhäsalmi mine (Inmet Mining Corporation), located in the town of Pyhäjärvi, central Finland. The mine produces copper, zinc and sulfur, and the concentration is performed in three consecutive flotation circuits. One centralized XRF analyzer (Outotec Courier® 6 SL) is normally used to monitor the slurry contents at the plant. The XRF analyzer is regularly calibrated based on laboratory analysis of slurry samples, and it measures the mass percentage values of iron, copper and zinc.

2.1 Process

The Pyhäsalmi ore contains mainly pyrite (FeS_2), sphalerite ($Zn_XFe_{1-X}S$), chalcopyrite ($CuFeS_2$) and pyrrhotite ($Fe_{1-Y}S$). The most important gangue minerals are barite and carbonates. The ore is mined underground, crushed

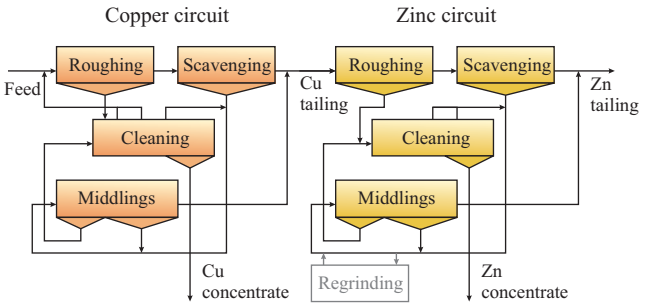

Fig. 1. The copper and zinc flotation circuits at Pyhäsalmi.

and hoisted to the concentration plant. The annual production of the mine is around 1.4 million tonnes.

The main flotation circuits of the plant are the copper and zinc circuits (Fig. 1), which extract chalcopyrite and sphalerite, respectively. Both circuits consist of roughing, scavenging, middlings flotation and cleaning stages. The final copper tailing is used as the input for the zinc circuit, and the final zinc tailing is further processed in sulfur circuit to separate pyrite.

2.2 VNIR Analyzer Prototype

The slurry VNIR spectrum analyzer prototype has been developed in several stages (Haavisto et al., 2008; Haavisto and Kaartinen, 2008), and the latest version currently in use at Pyhäsalmi is presented in the following for the first time. Figure 2 shows the structure and installation setup of the analyzer. The primary sampling slurry flows bring continuous samples from each process flow to the centralized XRF analyzer. The XRF analyzer samples these flows one by one and measures the elemental contents of the sample. For the slurry VNIR analysis, additional large jet flow cells are installed directly in the primary sample flows right before the secondary XRF sampling. With respect to the older prototypes, where a separate slurry flow was sampled from the primary XRF sample flow for the VNIR analysis, this more direct approach has two main advantages: 1) the last sampling stage is omitted, which improves the representativeness of the slurry sample, and 2) the blockage problems resulting from the additional sampling are avoided.

The jet flow cells are designed to produce a representative sample of the slurry in front of a sapphire glass window. The VNIR reflectance spectrum of the slurry is measured through the window by a fiber-optical spectrograph. In each slurry line, a protective housing surrounds the measurement equipment which consists of a halogen lamp for illumination, a collimator lens with an optical fiber for the VNIR measurement and a web camera for monitoring purposes. In addition, a minor instrument air flow is blown on the window to prevent condensation.

The common end of the optical fiber bundle is connected to a prism-grating-prism spectrograph (Specim ImSpector V10) (Aikio, 2001) equipped with an ordinary grayscale camera. The spectrograph collects and disperses light from the fiber bundle so that a single frame captured by the camera contains the spectral information of the light from all the fibers. An ordinary desktop computer is further

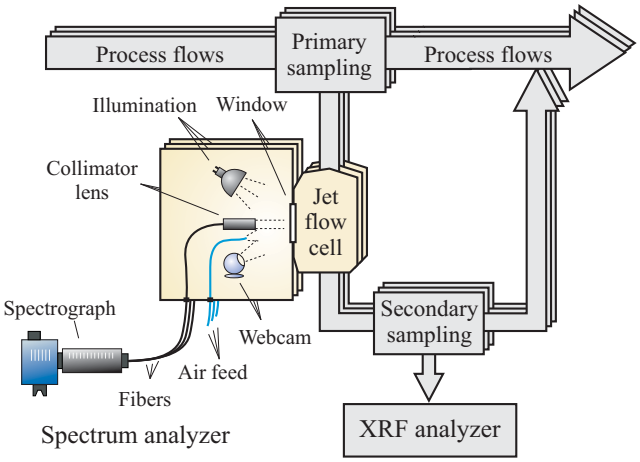

Fig. 2. The slurry VNIR spectrum analyzer prototype is installed directly on the primary sample flows of the XRF analyzer.

used to process the captured images and to calculate the content information as described in the following.

2.3 Data

The presented VNIR spectral assaying of the mineral slurries depends on the regular on-line calibration with the XRF assays. For this purpose, the XRF measurements are collected as soon as they are available from the XRF analyzer and the spectrum measurement is recalibrated after every new XRF sample.

In this article, the operation of the VNIR-based assaying method is demonstrated in the final copper and zinc concentrates of the Pyhäsalmi concentration plant. The XRF sampling interval is around 10 minutes for the copper concentrate, which is assayed twice during the XRF cycle, and around 19 minutes for the zinc concentrate, which is assayed once during the XRF cycle. However, the sampling can occasionally be irregular because of disturbances in the operation of the analyzer. Iron (Fe), copper (Cu) and zinc (Zn) are the primary elements measured. The VNIR spectra are measured with a sampling interval of five seconds, but some averaging is performed to match the VNIR measurements with the XRF samples. The final VNIR sampling rate is ten seconds.

For this study, a dataset from the copper and zinc final concentrates was collected during the normal operation of the plant in February 2009. Both datasets spanned two weeks and consisted of almost 121 000 VNIR spectra. The copper data contained 2154 XRF assays and the zinc data 1034 XRF assays. In the data preprocessing the reflectance data R were transformed to absorbance values ($\log(1/R)$) and the XRF data were scaled to unit variance. An additional constant predictor variable was used to compensate for the non-zero means.

3. ADAPTIVE CALIBRATION

The partial least squares (PLS) calibration method (Wold et al., 2001), which is a commonly used technique to analyze high-dimensional spectral measurements in chemometrics (Gemperline, 2006), is applied in this study. The

PLS model is formed using a set of calibration data samples, i.e., pairs of VNIR spectrum and XRF elemental content vectors measured from the same slurry sample. The model can then be used to predict the unknown elemental contents for new spectra.

However, a fixed calibration model is not adequate in continuous process use, since also other properties of the slurry (e.g. the particle size and mineral composition) affect the shape of the spectrum (Haavisto et al., 2008). These properties are mainly dominated by the source and mixture of the incoming ore as well as the grinding process, and can be assumed to change somewhat smoothly.

3.1 Recursive PLS

The recursive exponentially weighted PLS (rPLS) (Dayal and MacGregor, 1997b) is utilized to adaptively update the calibration model between the VNIR spectrum and the elemental contents. The rPLS approach is essentially based on the exponentially weighted recursive updating of the (unscaled) data covariance matrices:

$$R_{xx}(t_k) = \lambda R_{xx}(t_{k-1}) + x(t_k)x^T(t_k) \quad \text{and} \tag{1}$$

$$R_{xy}(t_k) = \lambda R_{xy}(t_{k-1}) + x(t_k)y^T(t_k), \tag{2}$$

where R_{xx} is an estimate of the predictor covariance matrix and R_{xy} an estimate of the cross-covariance matrix of the predictors and responses. The predictor column vector $x(t_k)$ contains the VNIR spectrum and the response column vector $y(t_k)$ the corresponding elemental content information from the XRF analyzer, each measured at the time t_k. The index k refers to the number of the XRF sample, and the forgetting factor λ, $0 < \lambda < 1$, determines how quickly the old data are discounted.

The up-to-date PLS calibration model $B(t_k)$ is calculated from the updated covariance matrices (1) and (2) with the fast kernel PLS algorithm introduced by Dayal and MacGregor (1997a). The obtained calibration model is then used to predict the elemental contents for the following VNIR spectra:

$$\hat{y}(t_k + \kappa T_\mathrm{s}, t_k) = B(t_k)x(t_k + \kappa T_\mathrm{s}), \tag{3}$$

where $T_\mathrm{s} = 10$ s is the sampling interval of the VNIR spectrum and the index κ is the number of the obtained VNIR spectrum samples after the calibration at t_k. The first index of the predicted value $\hat{y}$ indicates the time stamp of the VNIR spectrum, $t_k + \kappa T_\mathrm{s}$, and the second corresponds to the time the calibration model was calculated, t_k.

The operation of the adaptive calibration can be summarized as follows:

(1) When a new XRF sample $y(t_k)$ is measured at t_k, select the corresponding VNIR spectrum $x(t_k)$ and update the covariance matrices (1) and (2).
(2) Calculate the new PLS model matrix $B(t_k)$ using the up-to-date covariances.
(3) Use $B(t_k)$ to predict the slurry contents from the measured VNIR spectra with (3) until the next XRF assay is obtained at t_{k+1}.

3.2 Model precision

The precision of the VNIR assay relative to the XRF analyzer can be estimated by investigating the errors between the VNIR assays and the corresponding elemental contents measured by the XRF analyzer. For example, the error of the current VNIR value calculated with the previous model $B(t_{k-1})$ is:

$$\begin{aligned} e(t_k, t_{k-1}) &= \hat{y}(t_k, t_{k-1}) - y(t_k) \\ &= B(t_{k-1})x(t_k) - y(t_k). \end{aligned} \tag{4}$$

This precision evaluation is sound as long as the data point $\{x(t_k), y(t_k)\}$ is not used to calibrate the model $B(t_{k-1})$ that is being validated.

To describe the precision at an arbitrary time $t_k + \kappa T_\mathrm{s}$, the error is assumed to follow a normal distribution with zero mean:

$$e(t_k + \kappa T_\mathrm{s}, t_k) \sim N\left(0, \sigma^2(\kappa T_\mathrm{s}, t_k)\right), \tag{5}$$

where the variance of the distribution is a linear function of the calibration model update time t_k and the time elapsed from the previous recalibration κT_s:

$$\sigma^2(\kappa T_\mathrm{s}, t_k) = a(t_k)\kappa T_\mathrm{s} + b(t_k). \tag{6}$$

Basically this means that as more time elapses from the latest recalibration, the error variance is assumed to linearly increase. This assumption was detected to approximately hold for the used data. The parameter $a(t_k)$ represents the increase rate of the variance, and $b(t_k)$ gives the error variance immediately after the calibration step at t_k for model $B(t_k)$.

The parameters $a(t_k)$ and $b(t_k)$ are recursively estimated for each new calibration sample $\{x(t_k), y(t_k)\}$. Initially, the squared errors of the K previous calibration models for the new sample are calculated:

$$\left\{e^2(t_k, t_{k-1}), e^2(t_k, t_{k-2}), \ldots, e^2(t_k, t_{k-K})\right\}. \tag{7}$$

The momentary estimates $a^*(t_k)$ and $b^*(t_k)$ for the error model (5) parameters are obtained by least squares fitting a line to the squared errors (7). The momentary error deterioration rate, $a^*(t_k)$, is the complement of the line slope, and the momentary error variance immediately after recalibration, $b^*(t_k)$, is the line value at t_k. Figure 3 illustrates the point. If a negative value for either parameter is obtained, a zero is used instead.

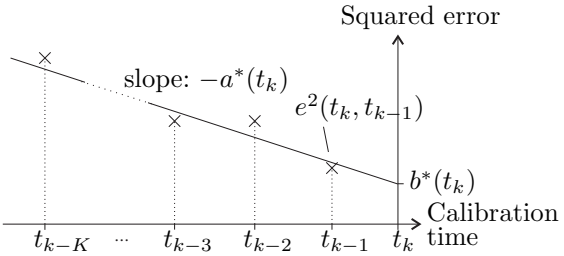

Fig. 3. The momentary error distribution parameters are obtained by fitting a line to the squared prediction errors calculated with the latest K calibration models.

The final parameter estimates $\hat{a}(t_k)$ and $\hat{b}(t_k)$ are formed as exponentially filtered values of the momentary parameters to obtain a smoothly behaving estimate for the error distribution:

$$\hat{a}(t_k) = \lambda_e \hat{a}(t_{k-1}) + (1 - \lambda_e)a^*(t_k), \tag{8}$$

$$\hat{b}(t_k) = \lambda_e \hat{b}(t_{k-1}) + (1 - \lambda_e)b^*(t_k). \tag{9}$$

For simplicity, the exponential filtering factor λ_e can be selected to match the one used in rPLS: $\lambda_e = \lambda$. Once the error distribution (5) is known, the confindence limits for the VNIR estimate error can easily be calculated.

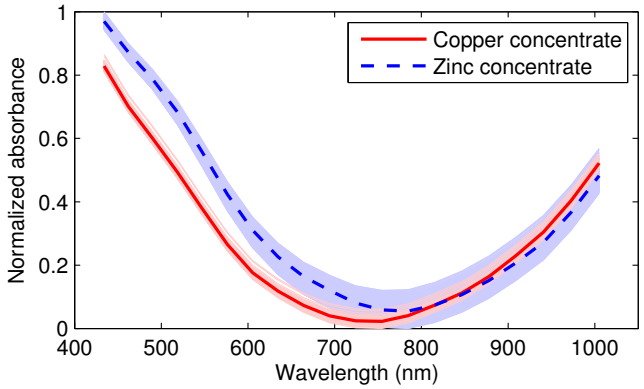

Fig. 4. Spectra of the zinc and copper concentrates during the analysis periods. *thick lines*: average spectra, *lighter regions*: the individual spectra.

It is important to note, however, that the error (4) does not directly tell how well the VNIR assay measures the real elemental contents of the slurry. This is because the VNIR assays are calibrated with the XRF results that also contain errors, typically both random (resulting from limited measurement time, noise, etc.) and systematic (resulting from imperfect calibration of the XRF analyzer). Therefore, the precision considerations presented above merely describe the ability of the VNIR prototype to predict the assays that the XRF analyzer would give for the same slurry samples.

4. RESULTS AND DISCUSSION

The operation of the VNIR spectrum slurry analyzer is demonstrated in the final copper and zinc concentrate slurry lines of the Pyhäsalmi concentration plant. The most important elemental measurements of the lines are the zinc and copper percentages, meaning that the VNIR analyzer should be able to detect the amount of sphalerite and chalcopyrite in the slurry.

4.1 General properties of the slurries

During the analysis periods, the average elemental contents for the copper concentrate slurry were 27.7% copper and 1.7% zinc, and for the zinc concentrate 1.3% copper and 50.0% zinc. Figure 4 shows the measured VNIR spectral data for the copper and zinc concentrate slurries. Clearly the different mineral contents of the two slurries result in distinguishable average spectra, and the grade variations in both slurry lines are seen as smaller changes around these averages.

The rPLS algorithm was applied to the measured data and the dynamic error distribution parameters (6) were calculated after each calibration step. The parameter values were $\lambda = \lambda_e = 0.95$ and $K = 10$. Initialization of the rPLS algorithm was performed during the first $n = 150$ XRF assay samples, which were then omitted from the subsequent analysis. The precision of the VNIR assays with respect to the XRF results was evaluated according to the error distribution (5) parameters. The averages of the parameters are given in Table 1 as the average increase rate $\bar{a}$ and the average standard deviation $\sqrt{\bar{b}}$. Also the relative values with respect to average slurry grades are calculated so that the precision of the different measurements can be compared.

Table 1. Averages of the estimated VNIR error distribution (5) parameters for the data sets.

Error parameter	Cu concentrate		Zn concentrate	
	Cu	Zn	Cu	Zn
Standard deviation $\sqrt{\bar{b}}$				
absolute value	0.43	0.082	0.22	0.62
relative to average grade	0.016	0.048	0.17	0.012
Increase rate $\bar{a}$				
absolute value (1/h)	0.21	0.0097	0.094	0.24
relative to average grade	0.0074	0.0057	0.075	0.0048

The largest relative error standard deviation is obtained for the copper grade measurement of the zinc concentrate, probably due to the small average copper grade. The larger copper and zinc grades of the copper and zinc concentrates, respectively, are measured with very good relative precision. Furthermore, even though small, the zinc grade of the copper concentrate slurry is captured with a small standard deviation. This is probably because of the higher overall reflectance of sphalerite (Haavisto and Kaartinen, 2008), which highlights the effect of zinc content variations in the VNIR spectrum.

The increase rates of the error variances are generally quite small, especially compared to the normal calibration period that is only in the range of 10–20 minutes. The effect of the increase factor is emphasized in cases where the XRF analyzer is temporarily out of operation, for example as a result of a maintenance break, and the next calibration of the rPLS model is delayed.

4.2 Examples

Copper concentrate: The operation and capabilities of the VNIR slurry spectrum analyzer are demonstrated by three case studies selected from the two collected data sets. Figure 5(a) illustrates the results of the analyzer on the copper concentrate slurry line with a five hour period of low-frequency grade oscillations. The figure shows the VNIR assays calculated directly from the measured spectra every 10 seconds, and a low-pass filtered version (90% exponential filtering) which better reveals the major changes in the grades. Also the original XRF measurements as well as the 95% confidence limits of the VNIR assay are given.

The grade oscillations could be detected from the XRF samples alone because of their low frequency. However, the VNIR assay reveals the grade changes more clearly and provides a practically continuous measurement of the grades. As a result of the low-pass filtering, the smoothed VNIR assay also avoids the sudden peak values in the grades, thus describing the overall behavior of the slurry contents more reliably. The XRF assays, on the other hand, are based on the sparse and short slurry samples, and only represent the instantaneous grade values. The confidence limits are drawn in Fig. 5 around the smoothed VNIR curve for clarity, even though they should actually be shown with respect to the original VNIR assay curve.

Zinc concentrate: A short interval of the zinc concentrate copper and zinc grades is shown in Fig. 5(b). Now the

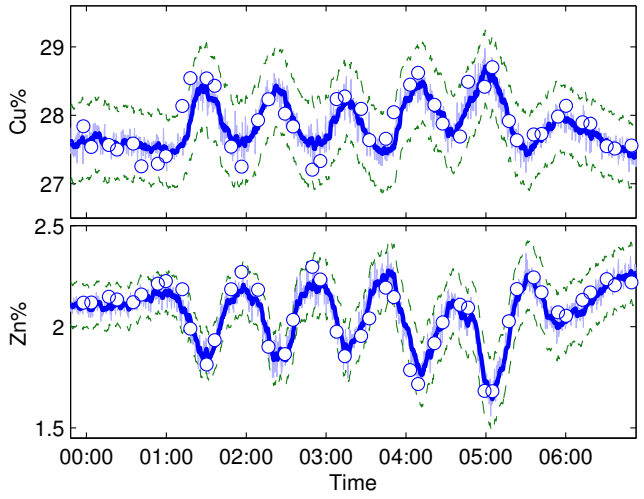

(a)

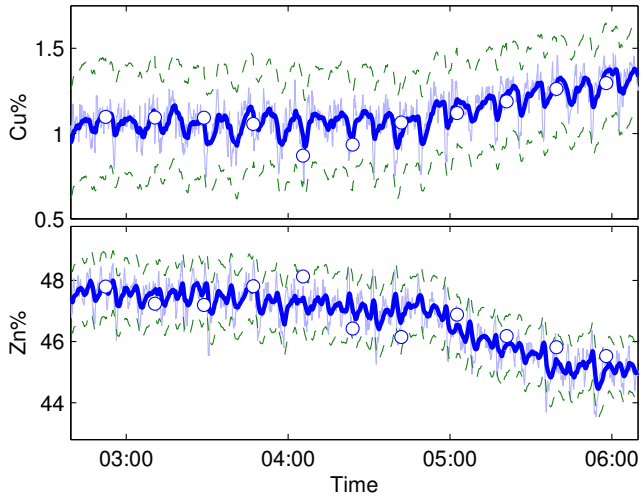

(b)

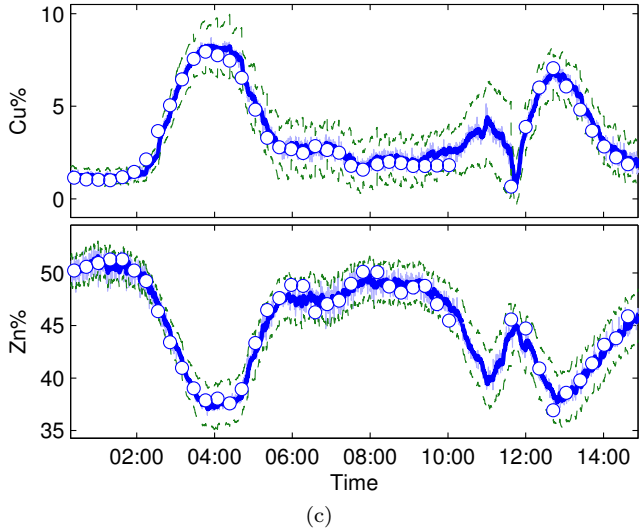

(c)

Fig. 5. The VNIR assays of zinc and copper showing (a) low-frequency oscillations in the copper concentrate, (b) high-frequency oscillations in the zinc concentrate and (c) major grade changes in the zinc concentrate. *Thin line*: VNIR assay; *thick line*: low-pass filtered VNIR assay; *dashed line*: 95% confidence limits; *circles*: XRF measurements.

XRF measurements do not show that any significant grade changes take place. However, the VNIR assays clearly indicate that a regular oscillatory behavior is present in both grade signals with a period of about 9 minutes. This kind of oscillation is most likely caused by a fluctuating slurry level in one of the zinc circuit flotation cells. The result demonstrates that the presented VNIR analyzer provides a method to detect also the higher-frequency oscillations directly in the final concentrate grades.

The second zinc concentrate example shown in Fig. 5(c) demonstrates the VNIR assay operation during large grade changes. Within the selected period the zinc grade drops a couple of times from the typical 50% to below 40% as a result of a process failure. The zinc VNIR assay is capable of following these changes and clearly indicates, for example, the start of the grade drop at 02:00-03:00 as well as the sharp increase just before 05:00. The copper assay, on the other hand, does not capture the first increase of the copper grade so well. This is happens because there is normally little variation in the copper grade of the zinc concentrate, and the adaptive calibration method gradually loses the information on the large copper values. However, after a few XRF samples with the increased copper grade, the calibration model adapts to the new situation. An improved calibration scheme based on several local models has been presented (Haavisto and Hyötyniemi, 2009) to increase the performance of the VNIR estimate during sudden grade changes.

The confidence limits in Fig. 5(c) clearly indicate how the variance of the error distribution increases in time between the XRF assays. Due to the process failure, the increase rate of the copper error distribution, in particular, is temporarily relatively high.

Another interesting point demonstrated in Fig. 5(c) is related to the period between 10:00 and 11:30. There the XRF analyzer has not been working, probably as a result of some maintenance operation. However, the VNIR slurry analyzer has continued to provide the assay information without interruption. Also the precision of at least the zinc assay has remained good, as indicated by the confidence limits and the first XRF measurement after the gap. Thus the VNIR assay can successfully replace the XRF analyzer for short periods of time.

4.3 VNIR assays in process monitoring and control

The zinc concentrate measurements of the VNIR slurry assay prototype have been available for the process operators at Pyhäsalmi almost since the start of the development work. After installation of the latest primary line prototype, the copper concentrate measurements proved to be reliable enough for real process usage as well. Currently, the low-pass filtered VNIR assays of both concentrate lines are displayed on the automation system screens for the use of the process operators. Additionally, arrows visualizing the direction and speed of the current grade change are shown on the screens as well. The top part of Fig. 6 illustrates the behavior of the arrow indicator during the zinc grade drop in the zinc concentrate. The color of the arrow highlights the rate of the change, thus better drawing the operator's attention to, for example, rapidly decreasing grade which may require manual control actions.

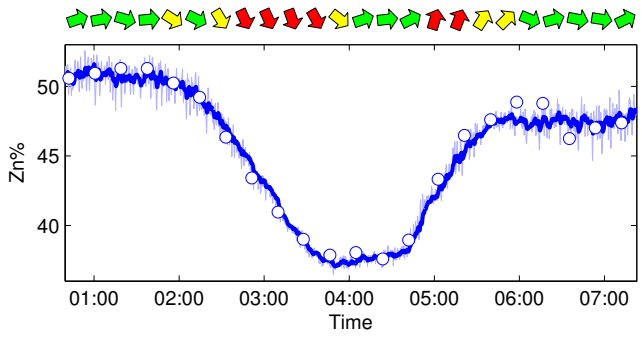

Fig. 6. A color-coded arrow indicator illustrates the grade change direction and rate (*green*: slow, *yellow*: moderate, *red*: rapid). *Thin line*: VNIR assay; *thick line*: low-pass filtered VNIR assay; *circles*: XRF assays.

According to an operator interview, the most important benefit of the improved assays is that the operators are able to see the grade changes between the sparse XRF measurement intervals. The new assays rapidly indicate the effect of the performed control actions and thus help the operators in process monitoring and control. Since the detection and correction of grade drops caused by process failures is faster, economical savings can also be obtained.

5. CONCLUSIONS

The usage of VNIR reflectance spectroscopy was presented in this study as a supplement for the traditional XRF slurry on-stream analyzer in assaying the zinc and copper concentrates of a mineral flotation circuit. The structure and installation of the VNIR reflectance spectrum analyzer prototype was presented. It was shown that a considerable decrease in sampling interval is achieved by the prototype for the copper and zinc assays when compared to the XRF analyzer. The VNIR measurement provides practically continuous estimates of the elemental contents in real time. The PLS calibration model is adaptively updated with a recursive algorithm and exponential forgetting. Furthermore, the precision of the VNIR assay with respect to XRF is estimated recursively. The VNIR analyzer was demonstrated to effectively capture the elemental content variations of the slurries in the case of major grade changes, as well as being able to replace the XRF analyzer for short time periods. In addition, both low-frequency and high-frequency grade oscillations can be detected.

ACKNOWLEDGMENTS

The support of Outotec Minerals Oy and Pyhäsalmi Mine Oy is gratefully acknowledged.

REFERENCES

Aikio, M. (2001). Hyperspectral prism-grating-prism imaging spectrograph. VTT Publications 435, Technical Research Centre of Finland.

Bartolacci, G., Pelletier Jr., P., Tessier Jr., J., Duchesne, C., Bossé, P.A., and Fournier, J. (2006). Application of numerical image analysis to process diagnosis and physical parameter measurement in mineral processes-part I: Flotation control based on froth textural characteristics. *Miner. Eng.*, 19(6–8), 734–747.

Dayal, B. and MacGregor, J. (1997a). Improved PLS algorithms. *J. Chemom.*, 7(3), 169–179.

Dayal, B. and MacGregor, J. (1997b). Recursive exponentially weighted PLS and its applications to adaptive control and prediction. *J. Process Control*, 7(3), 169–179.

De Waal, P. (2007). Tomorrow's technology — out of Africa — today. In *Proceedings of The Fourth Southern African Conference on Base Metals 2007*. Southern African Institute of Mining and Metallurgy, Swakopmund, Namibia.

Gemperline, P. (ed.) (2006). *Practical guide to chemometrics*. CRC Press, Boca Raton, FL, second edition.

Haavisto, O. (2009). Detection and analysis of oscillations in a mineral flotation circuit. *Control Eng. Pract.* Submitted.

Haavisto, O. and Hyötyniemi, H. (2009). Recursive multimodel partial least squares estimation of mineral flotation slurry contents using optical reflectance spectra. *Analytica Chimica Acta*, 642(1–2), 102–109.

Haavisto, O. and Kaartinen, J. (2008). Multichannel reflectance spectral assaying of zinc and copper flotation slurries. *Int. J. Miner. Process.* Submitted.

Haavisto, O., Kaartinen, J., and Hyötyniemi, H. (2006). Optical spectrum based estimation of grades in mineral flotation. In *Proceedings of the IEEE International Conference on Industrial Technology (ICIT 2006), Mumbai, India*, 2529–2534.

Haavisto, O., Kaartinen, J., and Hyötyniemi, H. (2008). Optical spectrum based measurement of flotation slurry contents. *Int. J. Miner. Process.*, 88(3–4), 80–88.

Hargrave, J.M. and Hall, S.T. (1997). Diagnosis of concentrate grade and mass flowrate in tin flotation from colour and surface texture analysis. *Miner. Eng.*, 10(6), 613–621.

Kaartinen, J., Hätönen, J., Hyötyniemi, H., and Miettunen, J. (2006). Machine-vision-based control of zinc flotation – a case study. *Control Eng. Pract.*, 14, 1455–1466.

Liu, J., MacGregor, J., Duchesne, C., and Bartolacci, G. (2005). Flotation froth monitoring using multiresolutional multivariate image analysis. *Miner. Eng.*, 18(1), 65–76.

McKee, D.J. (1991). Automatic flotation control - a review of 20 years of effort. *Miner. Eng.*, 4(7–11), 653–666.

Morar, S.H., Forbes, G., Heinrich, G.S., Bradshaw, D.J., King, D., Adair, B.J.I., and Esdaile, L. (2005). The use of a colour parameter in a machine vision system, SmartFroth, to evaluate copper floation performance at Rio Tinto's Kennecot copper concentrator. In G.J. Jameson (ed.), *Centenary of Flotation Symposium, Brisbane, Australia, 6–9 June 2005 - Proceedings*, 147–152. The Australasian Institute of Mining and Metallurgy.

Oestreich, J., Tolley, W., and Rice, D. (1995). The development of a color sensor system to measure mineral compositions. *Miner. Eng.*, 8(1/2), 31–39.

Wills, B.A. and Napier-Munn, T. (2006). *Wills' Mineral Processing Technology*. Butterworth-Heinemann, 7th edition.

Wold, S., Sjöström, M., and Eriksson, L. (2001). PLS-regression: a basic tool of chemometrics. *Chemom. Intell. Lab. Syst.*, 58, 109–130.